Journal of the Australian Ceramic Society (2021) 57:731–741
https://doi.org/10.1007/s41779-021-00579-0

RESEARCH

Fabrication and characterization of Al_2O_3-TiB_2 nanocomposite powder by mechanochemical processing

Hediye Aydin [1] · Benan Elmusa [1]

Received: 26 January 2021 / Revised: 2 February 2021 / Accepted: 10 February 2021 / Published online: 17 February 2021

Abstract

In order to synthesize alumina-titanium diboride nanocomposite powder, a mixture of titanium oxide, boron oxide, and aluminum powders was subjected to high-energy ball milling. The structural evaluation and the phase transformation of powder particles after different milling times were studied by X-ray diffractometry (XRD) and scanning electron microscopy (SEM). The results showed that only after 2 h of milling the Al/TiO/B_2O_3 reacted with a self-sustaining mode and an alumina-titanium diboride nanocomposite powder was formed. As far as we know, the fabrication of Al_2O_3-TiB_2 composite powder using a mechanochemical processing Al, TiO, and boron oxide as starting materials has not yet been studied, and also, milling was carried out for very long times to synthesize this powder. When similar studies on the subject are examined, in our study, TiO is used instead of TiO_2 as a titanium source, in synthesizing Al_2O_3-TiB_2 in situ nanocomposite powder. The critical benefit is that the replacement of elementary reagents by compounds usually leads to the formation of a structure with finer particles and requires a shorter milling time for the powder synthesis. In the final stage of milling, the crystallite size of alumina and titanium diboride was calculated to be less than 20 nm. The minimum particle size obtained in the particle size analysis was calculated as 0.0157 μm (15.7 nm). In FT-IR analyses, the peaks of Al-O bonds were between 409.16 and 673.91 cm^{-1} and that of Ti-B bonds were 739.03 and 740.45. It was determined to have 1017.9 and 1025.01 cm^{-1} peak values. The results showed that increasing the milling time up to 4 h has no significant effect other than reducing the crystallite size.

Keywords Al_2O_3-TiB_2 nanocomposite · Alumina · Titanium diboride · Mechanochemical processing

Introduction

Aluminum oxide (Al_2O_3) ceramics are among the most important ceramic materials used in electricity, optics, structural and biomedical applications due to their high melting point and abrasive resistance, perfect electrical insulation, low cost, and high chemical stability characteristics [1, 2].

However, the use of alumina-based ceramics by themselves is limited because of their low fracture toughness, low thermal shock resistance, and weak permeability. In order to improve these characteristics, alumina-based ceramics have been made into composites through the use of TiC, TiN, TiB_2, ZrO_2, SiC, etc. compounds as second phase [1].

✉ Hediye Aydin
hediye.aydin@dpu.edu.tr

[1] Department of Metallurgy and Material Engineering, Kütahya Dumlupinar University, 43100 Kütahya, Turkey

It has been reported that Al_2O_3 reinforced by tough secondary phases such as TiC, TiN, TiB_2, ZrO_2, and SiC has better hardness and mechanical characteristics compared with monolithic alumina [1–5]. Another probable mechanism to improve the mechanical properties of alumina-based ceramic matrix composites is reducing them to the nano-size [6].

TiB_2 has properties such as high abrasion strength, high strength, fracture toughness, high hardness, and good permeability. In addition, it also has chemical stability with its high abrasion strength and prefect thermal stability up to 1700°C [7]. Even though titanium diboride is preferred in many fields of industry due to its high hardness, its high density and difficulty in shaping reduce its workability. Hence, it is generally preferred to use TiB_2 as a composite instead of by itself. Al_2O_3-TiB_2 composite has stood out due to its various features such as high modulus of elasticity, abrasion resistance, and toughness in addition to its electrical properties. Al_2O_3-TiB_2 composite has attracted attention with its potential areas of use in the production of cutting tools, refractory materials, manufacturing of military armor, as well as its use in

applications that require corrosion and abrasion strength. It has been synthesized through methods such as hot pressing, pressureless sintering, pressureless metal infiltration (PRRIMX), direct metal oxidation method (DIMOX), self-propagating high temperature synthesis (SHS), and mechanochemical methods [6, 8–13]. All of these techniques cause heterogeneous microstructure which is important disadvantage. Additionally, the consolidation of the materials into a dense and high-strength body is difficult because of the strong covalent bonds and low self-diffusion coefficient of the constituent elements [14]. Mechanochemical synthesis is a solid-state reaction that is generally carried out without resorting to homogeneously distributed thermal or chemical procedures. The undesired reactions that develop due to melting and heterogeneity problems encountered during the classical alloying procedures can be eliminated by way of mechanochemical synthesis method.

Thereby, what can obtain synthesis material with a fine and homogenous structure in which one phase homogeneously dispersed in the other. The fact that it is low cost and has a wide range of application areas renders it advantageous [15]. It has been reported that it is quite efficient for chemical reactions induced via mechanochemical synthesis that can also be expressed as high-energy ball milling as well as for the production of materials such as nanocomposites [7]. Common reaction systems for preparing Al_2O_3-TiB_2 composites are Al-TiO_2-B, Al-TiO_2-H_3BO_3, Al-B_2O_3-Ti, Al_2O_3-Ti-B, and Al-TiO_2-B_2O_3 [1, 13]. The present work focuses on room temperature preparation Al_2O_3-TiB_2 nanocomposite powder using TiO instead of TiO_2 a novel approach of combining aluminum (Al), boron oxide (B_2O_3), and titanium oxide (TiO) as precursors. Also, in similar studies previously, Al_2O_3–TiB_2 nanocomposite powder was synthesized after 20, 30, 40, and 60 h of milling [16–19]. In this research, the possibility of mechanochemical synthesis of Al_2O_3–TiB_2 nanocomposite powder during short milling times. So, the low temperature and short milling times of the process has to be highlighted in this study. Thereby increasing the interest in this method enables low-cost material production when the performance-unit price is considered and ensures that the technique study in various other research subjects.

Materials and methods

Titanium oxide (TiO) (44 μm, 99.99% purity) and boron oxide (B_2O_3) (77 μm, 99.99% purity) and aluminum (Al) (40 μm, 99.99% purity) were used for composite synthesis. First, the mineralogical characterization of the materials was performed via X-ray diffraction analysis, whereas scanning electron microscope (SEM) was used for microstructure characterization prior to the experimental studies. Figure 1 presents the X-ray diffraction analysis results for the Al, B_2O_3, and TiO powders, whereas Fig. 2 shows the secondary electron images acquired from the initial powder surfaces via scanning electron microscope (SEM). As is shown in the SEM micrographs, titanium oxide (TiO) displays a tendency for agglomeration. Aluminum (Al) has an irregular structure, while boron oxide (B_2O_3) has an angular structure.

The starting materials were prepared with the lead of the main reaction provided below in order to obtain the Al_2O_3 and TiB_2 ceramic phase structure via mechanochemical synthesis. The weighing and milling for the starting powder mixtures were carried out in argon gas environment to provide an inert atmosphere. After filling the vial with powder and balls under argon atmosphere, milling was carried out in Retsch PM 200 planetary mill. Table 1 shows the milling parameters selected for the mechanochemical process.

XRD and FTIR (Bruker/Alpha) analyses were conducted in order to determine the impacts of the starting materials, synthesis of final products after mechanochemical procedure, and the reaction onset and formation with regard to synthesis. Panalytical, empyrean brand X-ray diffractometer device (Cu K_α radiation and Ni filter) was used, and the process was carried out under CuK_α radiation at a rate of 2°/min. Scans were performed between $10° < 2\theta < 80°$. The diffraction patterns obtained were compared with the standards determined by the "Joint Committee on Powder Diffraction and Standards (JCPDS)". The Scherrer formula was employed to estimate the crystallite size (d_{XRD}) from the strongest XRD reflection [20, 21]. Particle size analyses for the synthesis powders ground at different durations were performed using a Marvern brand Mastersizer. Pure water was used as dispersant during the measurements. Time-dependent surface area (BET- Nova Quantachrome) and mean particle size assessment were carried out during the experimental studies for the powders ground in the planetary mill. The analyses were performed in a 77 K medium with nitrogen adsorption. Scanning electron microscope (SEM- FEI Nova NanoSEM 650) studies were conducted in order to determine the morphological distribution of the powder mixtures obtained at the end of synthesis and especially the size distributions of the powders with a tendency for agglomeration.

Results and discussion

Phase evolution and reaction mechanism

As is stated in the relevant literature, it was predicted that the reactions between the starting powders will take place in 3 steps during milling. In the first step, 3α-Al_2O_3 and free boron element were formed following the reaction between $3B_2O_3$ and 6Al; in the second step, α-Al_2O_3 and free Ti were formed

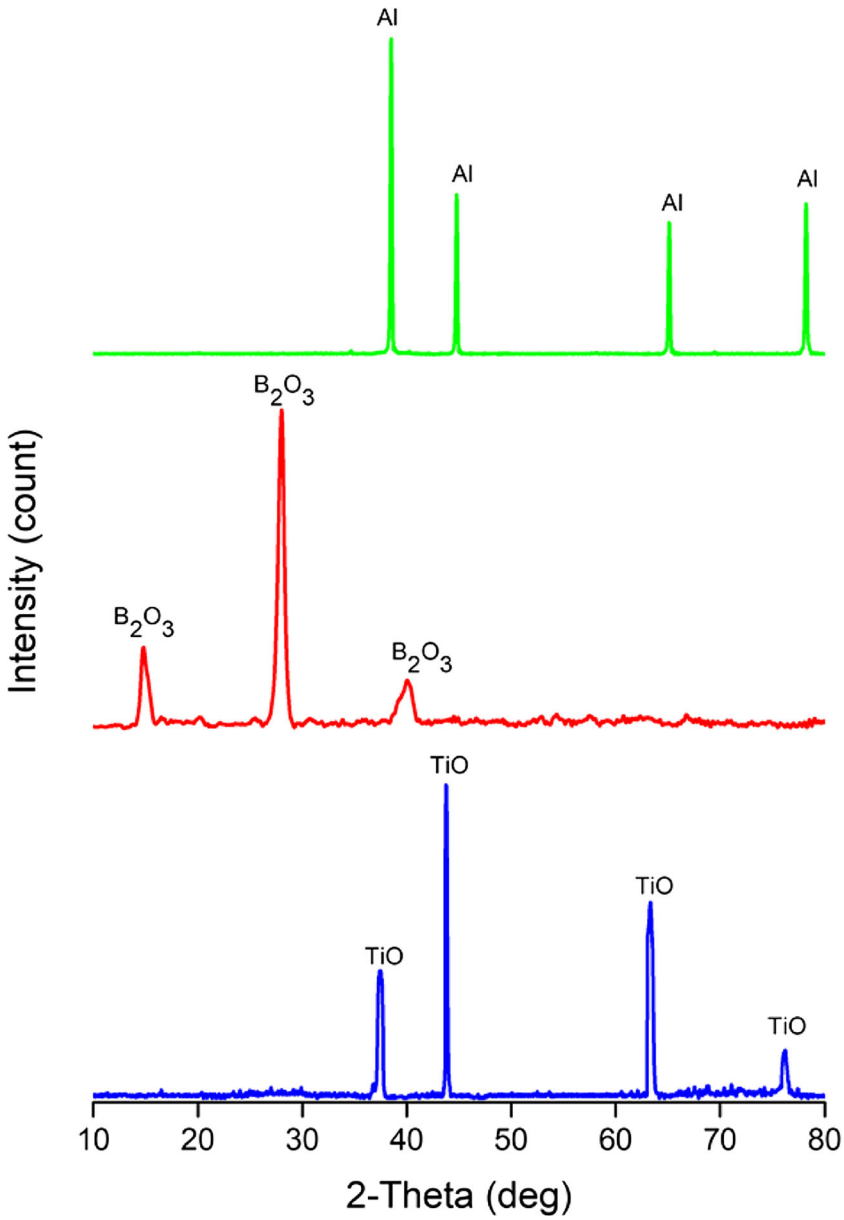

Fig. 1 XRD patterns of titanium oxide (TiO), boron oxide (B_2O_3), and aluminum (Al) powders

following the reduction of 3TiO by 2Al. It is considered the TiB_2 phase will form due to the reaction between elemental Ti and B. The thermodynamic evaluation of the reactions is provided below.

Reaction	Thermodynamic data	
	$\Delta H°_{298}$ (Kj/mol)	$\Delta G°_{298}$ (Kj/mol)
8 Al + 3 B_2O_3 + 3 TiO → 3 TiB_2 + 4 α-Al_2O_3	−2238.84	−2291.97
6 Al + 3 B_2O_3 → 3 α-Al_2O_3 + 6 B	−1217.1	−1174.35
2 Al + 3 TiO → α-Al_2O_3 + 3 Ti	−50.19	−158.97
3 Ti + 6 B → 3 TiB_2	−972.15	−959.7

According to thermodynamic parameters [22], the above reaction displays a high tendency towards being an exothermic reaction. The negative value of $\Delta G°_{298}$ suggests that reaction can thermodynamically take place at room temperature. This reaction is expected to continue as SHS [10]. According to literature [14], during the in situ formation of the Al_2O_3-TiB_2 composite, firstly alumina occurs due to the occurrence of thermite reactions, and the TiB_2 will occur, and the temperature rises to above 2300 °C.

It was observed when the XRD pattern for 1 h milling procedure was examined that the intensities of the peaks of B_2O_3 were lower compared with Al and TiO (Fig. 3). In addition, it was also observed that the α-Al_2O_3 and TiB_2 phase formations took place but that the transformations were not fully completed. Compared to the literature in which TiB_2

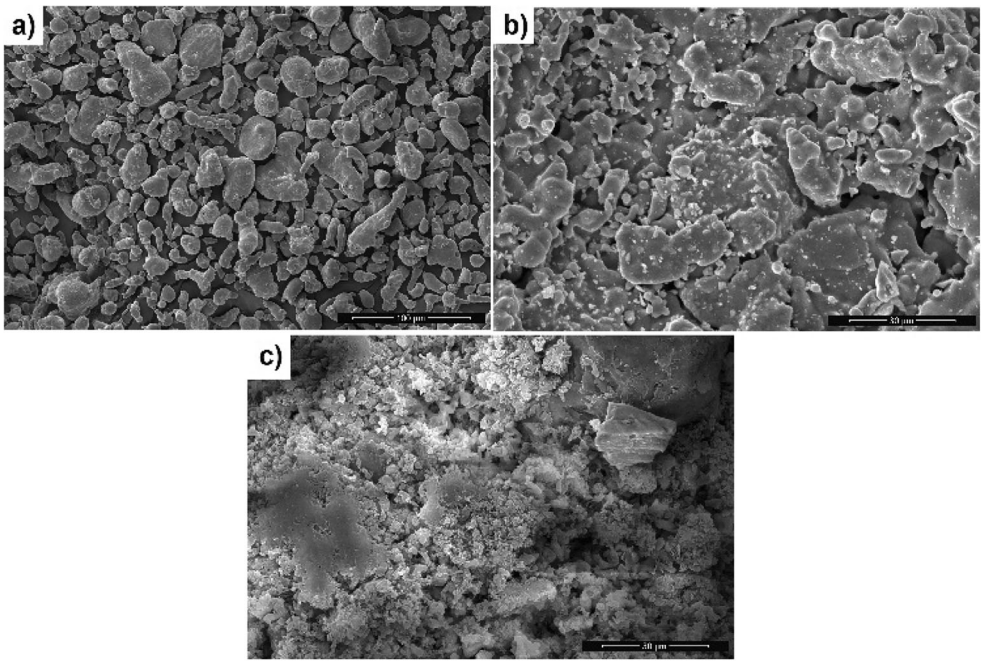

Fig. 2 SEM image of (**a**) Al, (**b**) B_2O_3, and (**c**) TiO powders

cannot form during the long-term milling processes of Al, B_2O_3, and different TiB_2 precursors.

In the present work, after a 1-h milling (BPR: 20/1 and rotational speed of vial: 600 rpm), the peaks of TiB_2 (JCPDS:98-004-4596) were appeared indicating the initiation of the reaction (Fig. 3). This is attributed to small-sized particles of the starting materials, the high speed of the milling rotation, and the high ratio of the balls to powder [23]. While the peaks for the B_2O_3 phase disappeared completely after the milling time was increased to 1.5 h, the intensities of the peaks for titanium oxide and aluminum were observed to decrease after 1.5 h of milling. Instead, two new broad peaks at about 43–45° were revealed which belong to α-Al_2O_3 (JCPDS:98-005-2647) and TiB_2 (JCPDS:98-004-4596) phases.

The reaction was completed in 2 h and no other peaks were observed other than those for α-Al_2O_3 and TiB_2 phases. According to the XRD pattern of powders milled for 2 h, the peaks of the starting material phases have been decreased and the peaks of Al_2O_3 and TiB_2 have remained. It can be said that the interfacial area of Al in contact with TiO and B_2O_3 increases as the milling time increases; hence the yield of the reactions increases as well [23]. Milling conditions justify this conspicuous variation. Increased milling energy, obtained by higher ball-to-powder weight ratio (BPR) and increased rotation speed, introduces more strain and expansion of the powder's defect concentration, thereby causing more readily amorphization [13].

Table 1 Parameters of mechanochemical synthesis

Rotation speed of vial (rpm)	600
Milling time (h)	1, 1.5, 2, 2.5, 3, 3.5, 4
Vial and ball material	Stainless steel
Capacity of vial (ml)	125
Diameter (mm) and number of balls	10 - 2 15 - 3 20 - 12
Powder/ball ratio	20:1

While a partial decrease was observed in the peak intensities for α-Al_2O_3 and TiB_2 after 2.5 h of milling, the TiB_2 peak intensity was observed to increase, and the peaks corresponding to Al_2O_3 were observed to decrease after 3 h of milling. Phase change was not observed in the patterns following 3.5 and 4 h of milling, with no structural changes observed except the broadening of the peaks following a decrease observed in the synthesis powders' crystallite size. The weakening of XRD peaks with increasing milling time beyond 2 h can be due to the crystalline phases' amorphization.

In a crystalline powder sample, when the crystallites' size becomes smaller than 0.005 μm (5 nm), the measured diffraction peak profile deviates from the same sample with its standard size of 0.5–10 μm in diameter. The uniform distribution of crystallites in all directions in a sample is also necessary for sufficiently reliable results for the diffraction peak profile. However, when the diameter of crystallites in a sample is less than 0.1 μm, the measured diffraction profiles "peak broadening" occurs. The reason for this is that the atomic plane's periodic region is limited, producing the same diffraction peak profile. Peak broadening can also occur by plastic deformation of the sample. This irregular deformation can be initiated by mechanical milling of the sample [24].

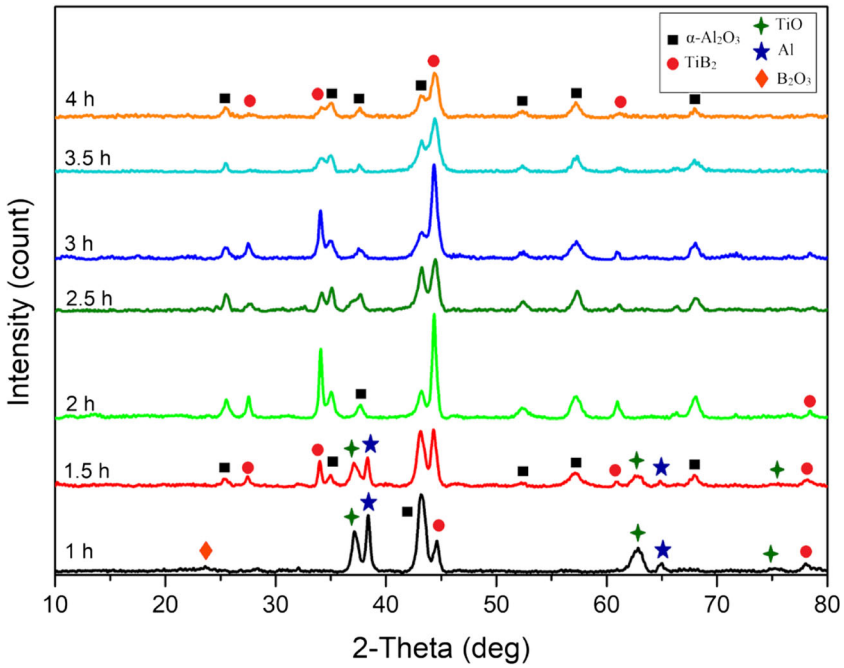

Fig. 3 XRD patterns of the Al_2O_3-TiB_2 powders after different milling times

As can be seen in Fig. 4, the main shift of these peaks and "peak broadening" is observed up to 1.5 h of intensive milling, which demonstrates the entrance of the starting materials in the lattice structures of alumina and TiB_2 that will also lead to the elimination of the starting materials peaks in the XRD patterns. By further increasing the milling time to 4 h, does not have any significant effect except a peak broadening and weakening of peaks can be seen. In fact, from the thermodynamic point of view, the system tends to reduce its internal energy.

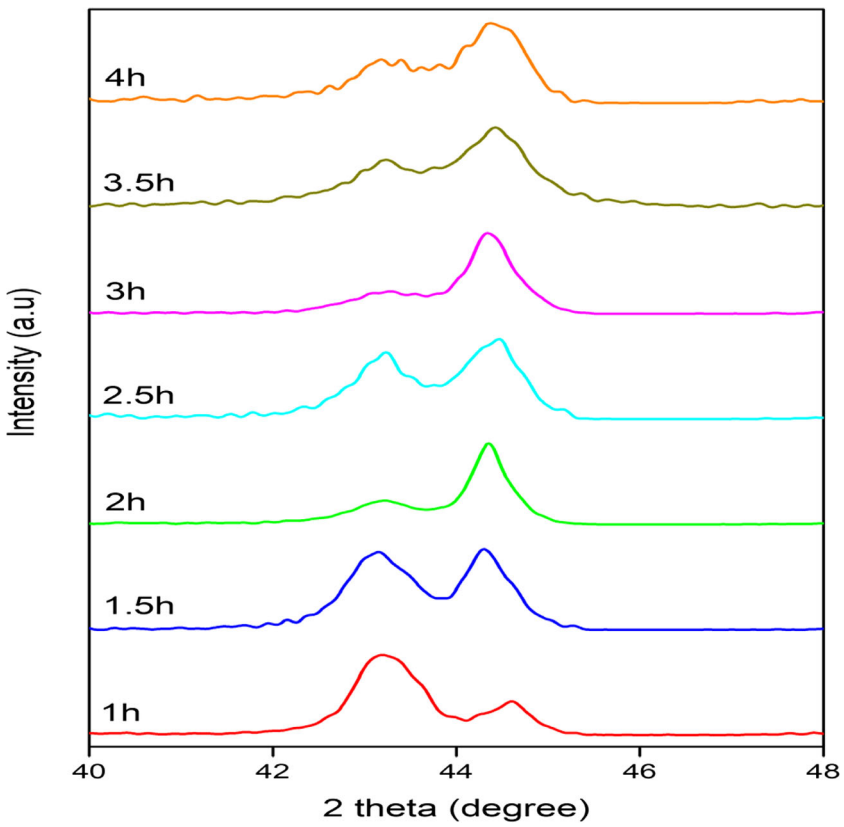

Fig. 4 The α-Al_2O_3 and TiB_2 peaks displacement during high-energy milling after 1, 1.5, 2, 2.5, 3, 3.5, and 4 h

These broad peaks indicate that new phases consist of a mixture of nano-metric and amorphous structures [21]. Also, the broadening and weakening of peaks are caused by the crystallite size reduction. Because of high background and very wide peaks, calculation of crystallite size by Williamson-Hall method is not possible [14]. In order to calculate the crystallite size in the synthesized composite powders, the Scherrer equation was used [21]. The peaks of maximum intensity were analyzed to determine the formation of new phases and the volume fraction.

$$D = \frac{K\lambda}{\beta \cos\theta}$$

Here, D represents the mean crystallite size, K is the Scherrer constant (0.9), λ is the X-ray wavelength (0.15406 nm), and β denotes the half peak width (radian) of the peak with maximum intensity, whereas θ is the XRD diffraction angle of the peak with maximum intensity. The determined amounts of average crystallite size for Al, B_2O_3, and TiO are 46.80, 9.12, and 25.13 nm, respectively. A continuous decrease was observed in the crystallite size of the samples subject to 1–4-h milling of Al_2O_3-TiB_2 nanocomposite powder. Al_2O_3-TiB_2 nanocomposite synthesized in short milling times results from the varying milling conditions. The calculated crystalline domain average size was 18.88 nm at a special peak of 35.14° (d104) for the α-Al_2O_3 and 16.50 nm at a special peak of 34.13° (d101) for the TiB_2. The mechanical deformation on the powder subject to increasing duration of milling at high speeds leads to a decrease in the crystal size while also resulting in a formation that approaches an amorphous structure due to crystalline errors. The structure that becomes stable due to the small particle size (high surface energy) and the formation of fractured surfaces creates a driving force for reactions.

Surface chemistry analysis

FT-IR analysis result for the powder subject to 2–3-h milling can be seen in Fig. 5. It was concluded following the FT-IR analysis evaluations for the powders subject to 2–3-h milling and heat treatment that peaks with wavelengths varying between 409.16 and 673.91 cm^{-1} which have formed due to the vibration movements of Al-O bonds [25–27].

It was determined that Ti-B bonds' peaks generally have values of 739.03; 740.45; 1017.9, and 1025.01 cm^{-1}, the values obtained from the analysis results are in accordance with the values indicated in literature [1, 28, 29].

Surface morphology analysis

Scanning electron microscope (SEM) was used to identify the morphological changes that take place subject to the milling times of the starting powder mixtures used in mechanochemical milling. SEM images were taken for the samples milled for 1 h up to 4 h. Figure 6 shows the microstructures of the composite powders synthesized via milling for 1–4 h. Based on the SEM image for the powder sample subject to milling for 1 h, it can be observed that the powders have adhered to each other and agglomerated (Fig. 6a). In this sample, while the ductile Al powder flattened with the impact of high speed milling environment, the B_2O_3 and TiO powders in the brittle structure were crumbled to pieces.

It can be stated that 1-h milled powders are more angular and also agglomerated (Fig. 6b). In general, a microstructure with a homogeneous powder size distribution could not be observed after milling for up to 1.5 h. It can be said that majority of the 2 h milled powders have a homogeneous size distribution (Fig. 6c). It can be put forth based on the SEM image that the particle sizes have reached nanometer values after obtaining Al_2O_3-TiB_2 (brittle-brittle) ceramic phase structure. It was observed when the SEM micrograph of the synthesis powders after 2.5 h milling was observed that hard agglomerates developed with increasing mean particle size (Fig. 6d) in addition to a particle size distribution with a wide range. The decrease in particle size attracted attention after 2.5 h milling. The particles started to become homogeneous transforming into more rounded spherical structures with increasing mechanical alloying time (Fig. 6e). As can be seen in Fig. 6 f and g, while the decrease in mean particle size of the powders continued for increasing milling times after 3 h, powder clusters that appear as a single particle structure

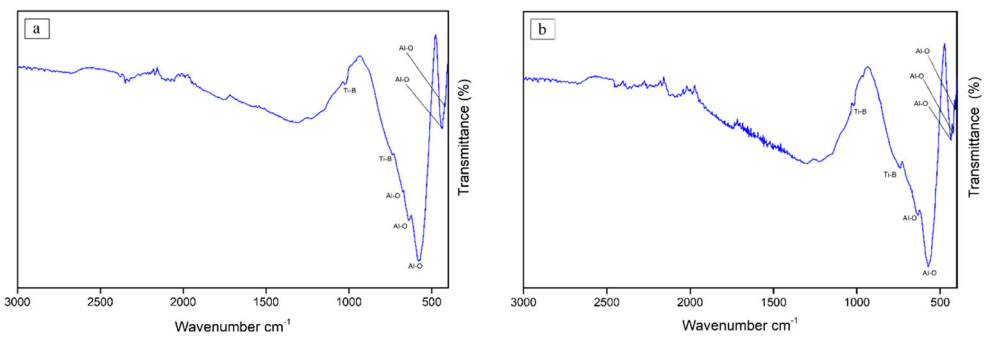

Fig. 5 (**a**) 2 h and (**b**) 3 h FT-IR spectra of samples after milling for 2–3 h

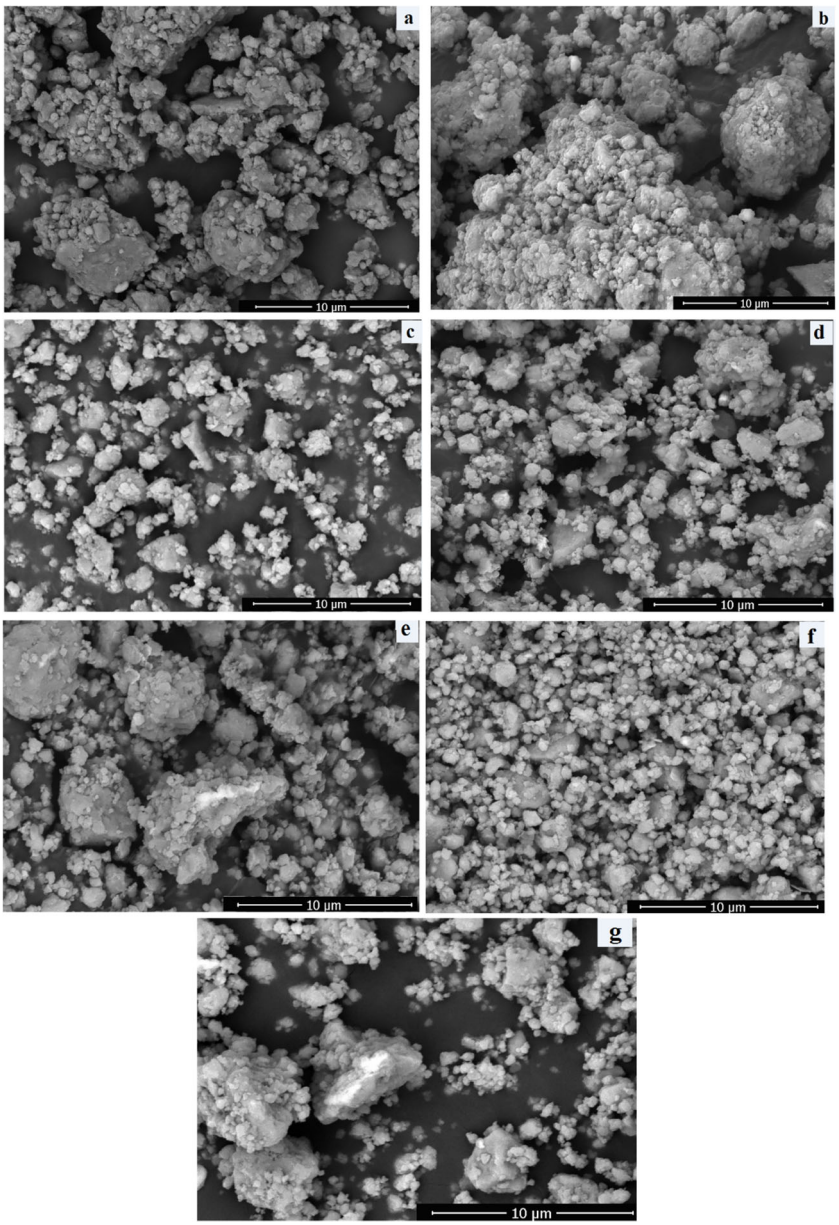

Fig. 6 (**a**–**g**) SEM images at ×10,000 magnification of Al_2O_3/TiB_2 powders milling for 1, 1.5, 2, 2.5, 3, 3.5, and 4 h, respectively

comprising nanometer-sized particles were observed which act as a driving force for sintering processes.

The number of non-bonded atoms on the surfaces increases due to the formation of powders with brittle surfaces along with the increasing milling time in the mechanochemical process. This leads to the agglomeration of powders with high surface energy leading to the formation of large, porous, and irregular powder clusters [1]. SEM image and corresponding EDS mapping analysis of the composite powders are given in Figs. 7 and 8. According to these figures, which indicate spectrum of Al_2O_3-TiB_2 composite powder with peaks of aluminum and titanium and also, this figure shows elemental distribution that confirms the presence of boron, aluminum, and titanium. The presence of the Fe peaks was caused by increasing the amount of Fe as contamination during milling.

Particle size analysis results

The variation in average particle size depending on time is given in Fig. 9. It was observed when the mean particle sizes of the starting powders were compared after 1–4 h mechanochemical milling procedures that there was a linear decrease in the mean particle sizes of the synthesis powders for up to 2 h, an increase tendency between 2 and 2.5 h followed by a decrease and no change between 3.5 and 4 h. Formation of small and large angled particle boundaries in the particle structure during mechanical deformation is among the factors that affects the decrease in particle size [1].

The decrease in mean particle size down to 15.7 nanometers especially after 2 h milling took place subject to the formation of the Al_2O_3-TiB_2 (brittle-brittle) ceramic phase.

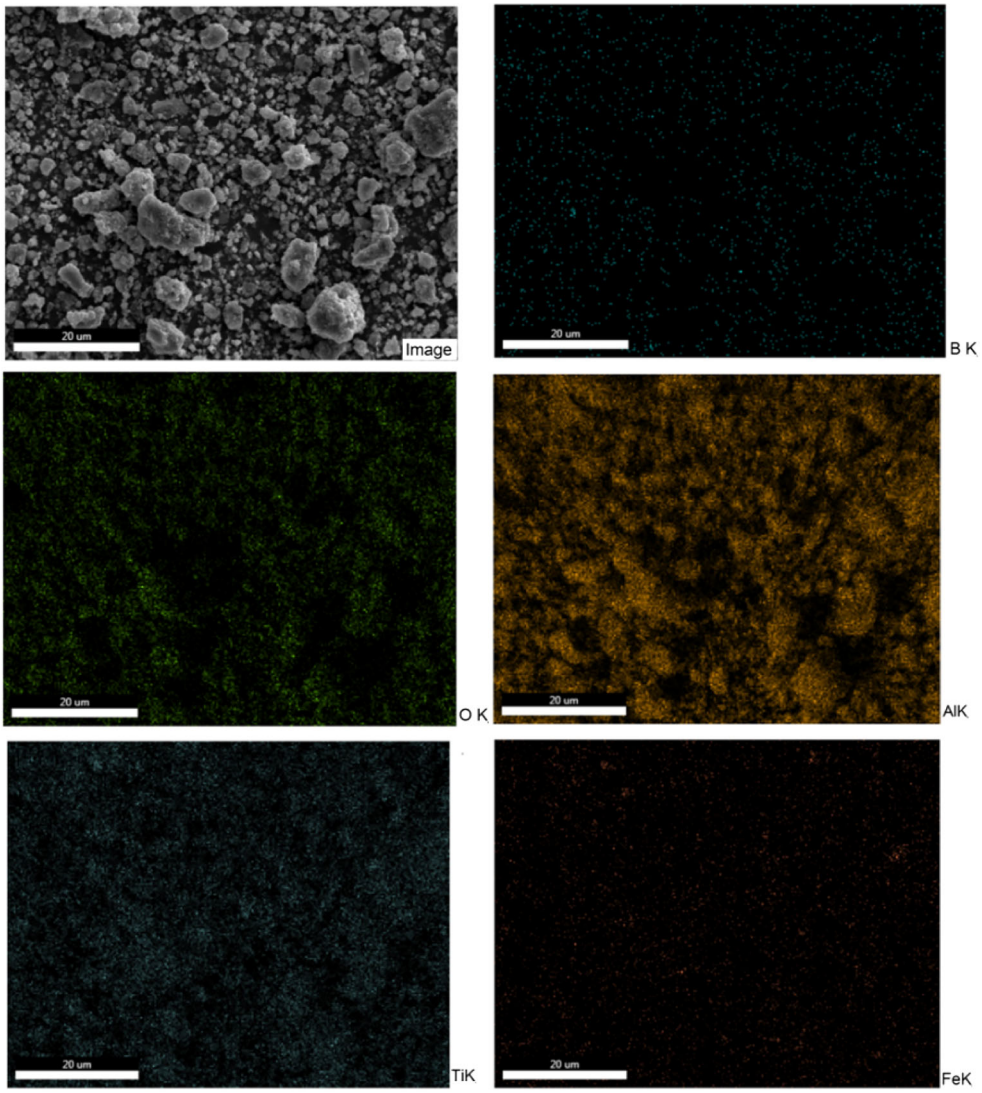

Fig. 7 SEM image of synthesized composite powder after milling for 2 h and EDS mapping of iron, titanium, aluminum, boron, and oxygen

Extensive plastic deformation increases the surface-volume ratio of the particles. There were no changes in mean size after the repeated continuation of cold welding (plastic deformation and agglomeration) and fracture (size reducer) mechanism throughout the 2–3.5 h milling period.

BET analysis results

Figure 10 shows the change in surface areas. The highest surface area determined based on BET analysis results was measured as 72.86 m^2/g for the sample milled for 2 h.

Surface area values were determined as 42.53 m^2/g after 1 h milling, 43.72 m^2/g after 1.5 h milling, 39.52 m^2/g after 2.5 h milling, 42.69 m^2/g after 3 h milling, 45.34 m^2/g after 3.5 h milling, and 45.70 m^2/g after 4 h milling. Mean particle size in BET analyses were calculated as ~1390 nm for 1 h milling, ~1190 nm for 1.5 h milling, ~15.7 nm for 2 h milling, ~1410 nm for 2.5 h milling, ~1250 nm for 3 h milling, ~1130 nm for 3.5 h milling, and ~1130 nm for 4 h milling. The changes in mean particle size obtained as a result of BET analyses are shown in Fig. 11.

Conclusions

The aim of the present study was to carry out the synthesis and characterization of the α-Al_2O_3-TiB_2 nanocomposite powder at room temperature via mechanochemical processing. First, Al, B_2O_3, and TiO powders were used as starting materials at room temperature conditions to successfully synthesize Al_2O_3-TiB_2 nanocomposite powder with high melting temperature via mechanochemical processing. The following results have been obtained as a result of experimental studies.

- Al_2O_3 and TiB_2 phase formations took place after 2-h milling. In conclusion, our experimental results confirm

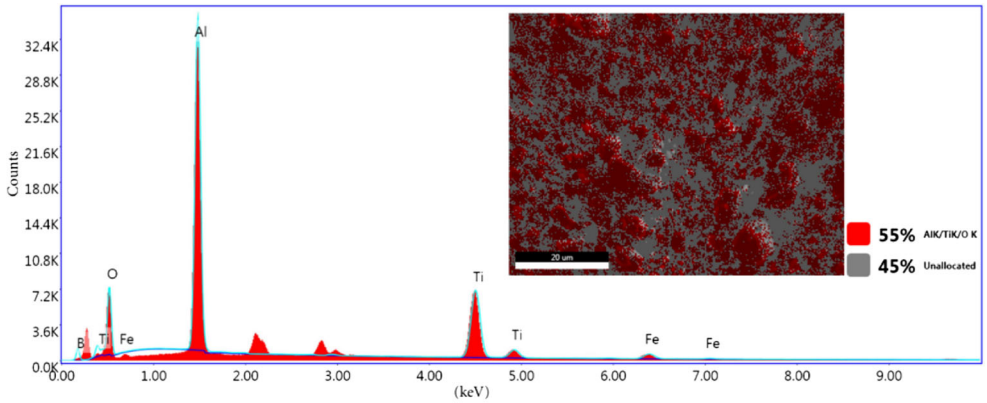

Fig. 8 EDX spectrum and elemental mapping of Al_2O_3-TiB_2 composite powder

Element	Sum Spectrum		AlK/TiK/O K		Unallocated	
	Weight %	Atomic %	Weight %	Atomic %	Weight %	Atomic %
BK	15.44	34.25	13.03	29.72	21.12	44.17
OK	10.46	15.68	10.42	16.06	10.92	15.43
AlK	34.44	30.62	38.03	34.77	24.12	20.21
TiK	33.88	16.97	33.19	17.09	36.43	17.20
FeK	5.79	2.48	5.33	2.35	7.41	3.00

that after 2 h of milling (BPR: 20/1 and rotational speed of vial: 600 rpm), the product is a high crystalline Al_2O_3-TiB_2 composite. While 2h milling process resulted in the gradual disappearance of the peaks for the starting materials as well as the actualization of the synthesis reaction, milling for more than 2 h led to the decrease in crystallite size.

- Widening of the XRD peaks can be attributed to the size of the crystals and the increase in the strain amount of the lattice generated due to the mechanochemical milling process. Therefore, the XRD analysis led to this conclusion that interactions in the Al-Ti-B system occur within the mill.
- Al-O and Ti-B peaks were identified in accordance with the peaks in both of the powder samples subject to FTIR analysis and milled for 2 and 3 h.
- The maximum mean particle size was calculated as 1410 nm for 2.5 h milling as a result of particle size distribution analysis. While the minimum particle size was obtained as 15.7 nm at the end of the 2 h milling procedure.
- The mean particle size was obtained at a minimum value of 15.7 nm as a result of the BET analysis result for 2 h milled powder. The highest surface area value was obtained as 72.86 m^2/g at the end of 2 h milling, and the lowest

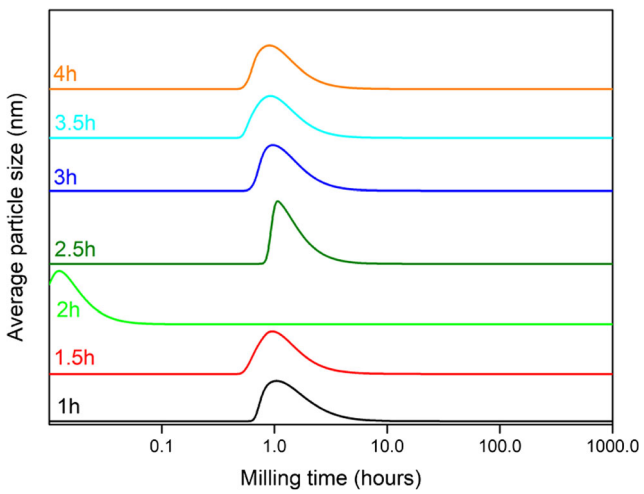

Fig. 9 Variation of the average particle size with milling time

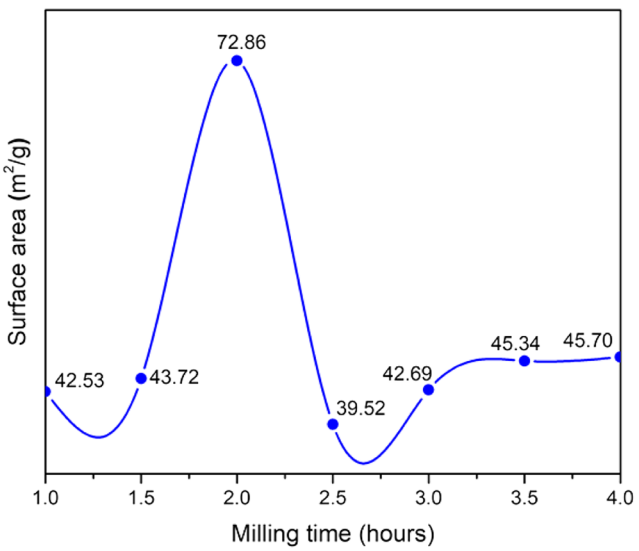

Fig. 10 Variation of the surface area with milling time

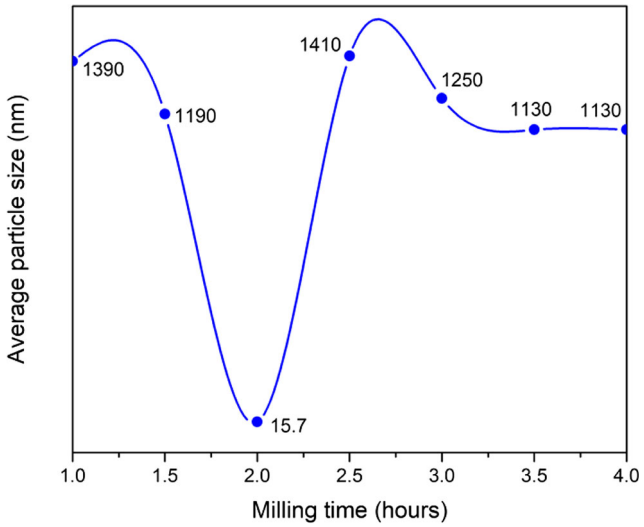

Fig. 11 Variation of the average particle size with milling time in mechanochemical synthesis

surface area value was identified as 39.52 m^2/g at the end of 2.5 h milling.

- When the microstructure characterization via SEM is taken into consideration in general, it can be observed that the particle morphology changed with the increase in mechanical alloying time and that the reinforcing phase and the matrix phase mixed together forming a homogeneous structure. In the other hand, both the Al_2O_3 and the TiB_2 are hard and brittle components, and during high-energy milling, their particle sizes reduced due to continuous fracturing. So, the particle size seems more homogeneous and finer after 2 h milling. It has been observed that the powders that look like a single particle have actually been formed with the agglomeration of nanometer-sized particles.

References

1. Benjamin, J.S.: Mechanical alloying A perspective. Metal Powder Rep. **45**, 122–127 (1990)
2. Al-Azzawi, A., Baumli, P., Mucsi, G.: Mechanical alloying and milling. Conference: İnternational Multidisciplinary Scientific Conference, University of Miskolc (2015). https://doi.org/10.26649/musci.2015.017
3. Lu, L., Lai, M.O., Wang, H.Y.: Synthesis of titanium diboride TiB_2 and Ti-Al-B metal matrix composites. J Mater Sci. **35**, 241–248 (2000)
4. Tuan, W.H., Chen, R.Z., Wang, T.C., Cheng, C.H., Kuo, P.S.: Mechanical properties of Al_2O_3/ZrO_2 composites. J Eur Ceram Soc. **22**, 2827–2833 (2002)
5. Xu, C., Ai, X., Huang, C.: Fabrication and performance of an advanced ceramic tool material. Wear. **249**, 503–508 (2001)
6. Gorlanov, E. S., Bazhin, V.Yu., Fedorov, S.N.: Low-temperature synthesis of titanium diboride. İX İnt. Congr. Non-Ferrous Metals Miner. 321–327 (2017)
7. Mohammad Sharifi, E., Karimzadeh, F., Enayati, M.H.: Synthesis of titanium diboride reinforced alumina matrix nanocomposite by mechanochemical reaction of Al-TiO_2-B_2O_3. J Alloys Compd. **502**, 508–512 (2011)
8. Subramanian Benjamin, J.S.: Dispersion strengthened superalloys by mechanical alloying. Metall Trans A. **1**, 2943–2951 (1970)
9. Kang, S.H., Kim, D.J.: Synthesis of nano-titanium diboride powders by carbothermal reduction. J Eur Ceram Soc. **27**, 715–718 (2007)
10. Karthiselva, N.S., Murty, B.S., Bakshi, S.R.: Low temperature synthesis of dense tib_2 compacts by reaction spark plasma sintering. İnt J Refract Metals Hard Mater. **48**, 201–210 (2015)
11. Ergin, N., Garip, Y., Özdemir, Ö.: Production of Ti-Al-B based composites by reduction combustion synthesis technique. Aku J Sci Eng. **14**, 489–492 (2014)
12. Baca, İ., Stelzer, N.: Adapting of sol-gel process for preparation of TiB_2 powder from low-cost precursors. J Eur Ceram Soc. **28**, 907–911 (2008)
13. Khaghani-Dehaghani, M.A., Ebrahimi-Kahrizsangi, R., Setoudeh, N., Nasiri-Tabrizi, B.: Mechanochemical synthesis of Al_2O_3-TiB_2 nanocomposite powder from Al-TiO_2-H_3BO_3 mixture. Int J Refract Met Hard Mater. **29**, 244–249 (2011)
14. Rabiezadeh, A., Hadian, A.M., Ataie, A.: Preparation of alumina/titanium diboride nano-composite powder by milling assisted sol-gel method. Int J Refract Met Hard Mater. **31**, 121–124 (2012). https://doi.org/10.1016/j.ijrmhm.2011.09.015
15. Li, S., Zhu, L., Liu, L., Chen, L., Li, H., Sun, C.: İnfluence of high-energy ball milling and additives on the formation of sphere-like α-Al_2O_3 powder by high-temperature calcination. Z. Naturforsch. Sect. B J. Chem. Sci. **73** (2018).
16. Nazari, A.G., Mozafari, M.: Simulation of structural features on mechanochemical synthesis Of Al_2O_3-TiB_2 nanocomposite by optimized artificial neural network. Adv Powder Technol. **23**, 220–227 (2012)
17. Mousavian, R.T., Sharafi, S., Shariat, M.H.: Preparation of nanostructural Al_2O_3-TiB_2 İn-Situ composite using mechanically activated combustion synthesis followed by intensive milling. İran J Mater Sci Eng. **8**, 1–9 (2011)
18. Sharifi, E.M., Karimzadeh, F., Ve Enayati, M.H.: Preparation of Al_2O_3-TiB_2 nanocomposite powder by mechanochemical reaction between Al, B_2O_3 and Ti. Adv Powder Technol. **22**, 526–531 (2011)
19. Rabiezadeh, A., Ataie, A., Hadian, A.M.: Mechano-Chemical Synthesis of TiB_2-Al_2O_3 Nano-composite by reaction between TiO_2, B_2O_3 and Al. Adv Mater Res. **488-489**, 955–959 (2012)
20. Pandey, V.K., Patel, B.P., Guruprasad, S.: Role of ceramic particulate reinforcements on properties and fracture behavior of aluminum - based composites. Mater Sci Eng. **745**, 252–264 (2019)
21. Dinnebier R.E., Billinge S.J.L.: Powder diffraction theory and practice Cambridge. (2008).
22. Kubaschewski, O., Alcock, C.B.: Metallurgical thermochemistry, 5th edn. Pergamon Press (1979)
23. Winterer, M.: Nanocrystalline Ceramics, p. 53. Springer, Berlin (2002)
24. Aydin, H., Goren, R., Koc, U.: Mechanochemical-assisted synthesis and characterization of Al_2O_3/B_4C ceramics. J. Aust. Ceram. Soc. 1–11 (2020)
25. Mikrajuddin, A., Khairurrijal, K.: Derivation of scherrer relation using an approach in basic physics course. J Nanosains Nanoteknol. **1**, 28–32 (2008)
26. Naayi, S.A., Hassan, A.İ., Salim, E.T.: FTIR and X-ray diffraction analysis of Al_2O_3 nanostructured thin film prepared at low temperature using spray pyrolysis method. İnt J Nanoelectron Mater. **11**, 1–6 (2018)
27. Prashanth, P.A., Raveendra, R.S., Hari Krishna, R., Ananda, S., Bhagya, N.P., Nagabhushana, B.M., Lingaraju, K., Raja Naika,

H.: Synthesis, characterizations, antibacterial and photoluminescence studies of solution combustion-derived α-Al_2O_3 nanoparticles. J Asian Ceram Soc. **3**, 345–351 (2015)
28. Liu, C., Shih, K., Gao, Y., Li, F., Wei, L.: Dechlorinating transformation of propachlor through nucleophilic substitution by dithionite on the surface of alumina. J Soils Sediments. **12**, 724–733 (2012)
29. John, S.K., Anappara, A.A.: Aqueous dispersions of highly luminescent boron-rich nanosheets by the exfoliation of polycrystalline titanium diboride. New J Chem. **43**, 9953–9960 (2019)